International Journal of Mechanical, Industrial and Aerospace Sciences
ISSN: 2517-9950
Vol:2, No:7, 2008

Laser Surface Hardening Considering Coupled Thermoelasticity using an Eulerian Formulations

Me. Sistaninia, G.H.Farrahi, and Ma. Sistaninia

Abstract**—**Thermoelastic temperature, displacement, and stress in heat transfer during laser surface hardening are solved in Eulerian formulation. In Eulerian formulations the heat flux is fixed in space and the workpiece is moved through a control volume. In the case of uniform velocity and uniform heat flux distribution, the Eulerian formulations leads to a steady-state problem, while the Lagrangian formulations remains transient. In Eulerian formulations the reduction to a steady-state problem increases the computational efficiency. In this study also an analytical solution is developed for an uncoupled transient heat conduction equation in which a plane slab is heated by a laser beam. The thermal result of the numerical model is compared with the result of this analytical model. Comparing the results shows numerical solution for uncoupled equations are in good agreement with the analytical solution.

Keywords**—**Coupled thermoelasticity, Finite element, Laser surface hardening, Eulerian formulation.

.

I. INTRODUCTION

THE primitive theoretical and experimental investigations of laser heating of materials date back to the 1960. Traditionally in these researches it was assumed that thermal and mechanical fields were uncoupled in the material [1-5]. In these investigations first the thermal fields due to laser irradiation on the surface were modeled and then the thermal results were used to find displacement field and stress profile. In recent years, considerable researches have been carried out on the numerical analysis of coupled thermoelasticity problems. Coupled thermoelasticity surround the phenomena which describe the elastic and thermal behavior of material. Many attempts have been done to solve the uncoupled thermoelasticity problems in steady or transient heat conduction states, but few investigations have been carried out successfully for coupled thermoelasticity problems [6].

Me. Sistaninia is with the Dept. of Mechanical Engineering, Sharif University of Technology, Tehran- Iran, (e_mail: sistaninia@gmail.com).

G.H. Farrahi is with the Dept. of Mechanical Engineering, Sharif University of Technology, Tehran- Iran, (e_mail: farrahi@sharif.ir).

Ma. Sistaninia is with the Dept. of Mechanical Engineering, Iran University science and Technology, Tehran- Iran, (e_mail: masoud1361@yahoo.com).

This paper considers coupled thermoelasticity to find thermoelastic temperature, displacement, and stress profile in Eulerian formulation.

Quasi-steady-state process is a process that is steady in either a stationary or a moving configuration. For uniform velocity and heat flux distribution, laser surface-hardening become a quasi-steady-state process and the Eulerian formulations leads to a steady-state problem. But Lagrangian formulations for such process remain transient and need a transient analysis. For solving transient problems numerically time-increment approach is used with a great number of increments. Also it is necessary to use dense mesh throughout the model length. Because of these reasons the run-time of Lagrangian analysis is much more than the run-time of Eulerian analysis so the analysis of a quasi-steady-state process using an Eulerian formulations is computationally efficient [7].

II. GOVERNING EQUATIONS

In this study, Galerkin's method is used to express the Euler energy balance equation in weak formulation. This equation is solved numerically using finite element discretization.

At, $t>0$ a semi infinite homogeneous, isotropic, thermoelastic solid is subjected to a moving Gaussian rectangular laser beam as shown in Fig. 1 Only a layer is considered which extends through $-b<y<b$ and $0<x<l$. The l and b are long enough so that can be assumed the initial conditions don't change on the boundary at $y=+b$,$y=-b$,and $x=0$, thus the layer is rigidly bonded along these bounds. The laser beam's energy is absorbed in the plane of the free surface and diffuses through the workpiece.

The governing equations for the dynamic coupled thermoelasticity in the absence of body forces can be written as follows [8]:

$$(\lambda+\mu)u_{j,ij}+\mu u_{i,jj}-\rho\ddot{u}_i-\gamma T_{,i}=0 \quad (1)$$

$$kT_{,ii}-\rho c\dot{T}-\gamma T_o\dot{u}_{j,j}=0 \quad (2)$$

where u_i, λ, μ, ρ , T, T_o, γ, k and c are the components of displacement vector, Lame's constants, density, absolute temperature, reference temperature, stress– temperature modulus, conductivity and specific heat at constant strain or volume that is equal to [9],

$$c = c_p - 3\frac{T_o}{\rho}\alpha\gamma \tag{3}$$

where c_p is specific heat at constant stress or pressure (notice that for uncouple thermoelasticity $c=c_p$) and α is linear thermal expansion coefficient.
It is convenient to introduce the dimensionless variables as follows [6]:

$$\hat{x} = \frac{x}{\upsilon}; \qquad \hat{t} = \frac{tC_s}{\upsilon}; \qquad \hat{\sigma}_{ij} = \frac{\sigma_{ij}}{\gamma T_o};$$
$$\hat{u}_i = \frac{(\lambda+2\mu)u_i}{\upsilon\gamma T_o}; \qquad \hat{T} = \frac{T-T_o}{T_o} \tag{4}$$

where $\upsilon = k/\rho c C_s$ is the dimensionless unit length and $C_s = \sqrt{(\lambda+2\mu)/\rho}$ the velocity of propagation of the longitudinal wave. Eqs. (1) and (2) is taken the form

$$\frac{\mu}{\lambda+2\mu}\hat{u}_{i,jj} + \frac{\lambda+\mu}{\lambda+2\mu}\hat{u}_{j,ij} - \hat{T}_{,i} - \ddot{\hat{u}}_i = 0 \tag{5}$$

$$\hat{T}_{,ii} - \dot{\hat{T}} - C\dot{\hat{u}}_{j,j} = 0 \tag{6}$$

C is coupling parameter and is equal to,

$$C = \frac{T_o\gamma^2}{\rho c(\lambda+2\mu)} \tag{7}$$

For the two-dimensional domain, these equations reduce to:

$$\begin{cases} \left(\frac{\bar{\mu}}{(\bar{\lambda}+2\mu)}\Delta + \frac{(\bar{\lambda}+\mu)}{(\bar{\lambda}+2\mu)}D_1^2\right)\hat{u}_1 + \left(\frac{(\bar{\lambda}+\mu)}{(\bar{\lambda}+2\mu)}D_1D_2\right)\hat{u}_2 - \ddot{\hat{u}}_1 - D_1\hat{T} = 0 \\ \left(\frac{(\bar{\lambda}+\mu)}{(\bar{\lambda}+2\mu)}D_1D_2\right)\hat{u}_1 + \left(\frac{\mu}{(\bar{\lambda}+2\mu)}\Delta + \frac{(\bar{\lambda}+\mu)}{(\bar{\lambda}+2\mu)}D_2^2\right)\hat{u}_2 - \ddot{\hat{u}}_2 - D_2\hat{T} = 0 \\ -(CD_1)\dot{\hat{u}}_1 - (CD_2)\dot{\hat{u}}_2 + \Delta\hat{T} - \dot{\hat{T}} = 0 \end{cases} \tag{8}$$

where $D_i = \partial/\partial\hat{x}_i$ (i=1,2) and Δ denotes the Laplacian. under plane strain assumptions $\bar{\lambda}$ and $\bar{\gamma}$ can be related to the Lame′ constants λ , μ and stress–temperature modulus, γ =(3λ+2μ)α , as [10],

$$\bar{\lambda} = \lambda \quad \text{and} \quad \bar{\gamma} = \gamma \tag{9}$$

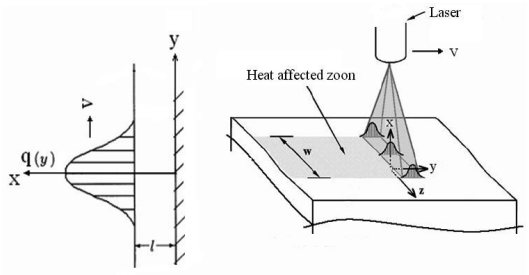

Fig. 1 Schematic of a material subjected to thermal load from moving Gaussian rectangular laser beam.

In Eulerian formulations the reference configuration is a control volume through that the workpiece moves. The derivative of variables (temperature and displacement) with respect to time in the moving body are given by,

$$\frac{dU_i}{dt} = \frac{\partial U_i}{\partial t} + \frac{\partial U_i}{\partial x_j}\frac{dx_j}{dt} \qquad (i=1,2,3) \tag{10}$$

Where $U_i = [u_1\ u_2\ T]$ and x_j (j=1,2) is the material system co-ordinate, which moving with a velocity ***v*** in space. Hence equations (10 can be expressed as

$$\frac{dU_i}{dt} = \frac{\partial U_i}{\partial t} + \mathbf{v}.\nabla U_i \tag{11}$$

And also the second derivative of displacement in the flowing body with respect to time is given by:

$$\frac{d^2u_i}{dt^2} = \frac{\partial V_i}{\partial t} + \mathbf{v}.\nabla V_i \qquad (i=1,2) \tag{12}$$

Where $V_i = \left[\frac{du_1}{dt} \quad \frac{du_2}{dt}\right]$ and $\nabla = e_m\frac{\partial}{\partial x_m}$ (m=1,2)
Since the control volume has a steady-state temperature and displacement profile for, the equations (11,12) for a quasi-steady-state process reduce to:

$$\frac{dU_i}{dt} = \mathbf{v}.\nabla U_i \qquad (i=1,2,3) \tag{13}$$

$$\frac{d^2u_i}{dt^2} = \mathbf{v}.\nabla V_i \qquad (i=1,2) \tag{14}$$

If the laser beam moves along y (or x_2) direction, (13, 14) simplifies as follows:

$$\frac{dU_i}{dt} = vD_2U_i \qquad (i=1,2,3) \tag{15}$$

$$\frac{d^2u_i}{dt^2} = v^2D_2^2u_i \qquad (i=1,2) \tag{16}$$

Substituting (15) and (16), in Eq. (8) yields

$$\begin{cases} \left(\frac{\mu}{(\lambda+2\mu)}\Delta + \frac{(\lambda+\mu)}{(\lambda+2\mu)}D_1^2\right)\hat{u}_1 + \left(\frac{(\lambda+\mu)}{(\lambda+2\mu)}D_1D_2\right)\hat{u}_2 - D_1\hat{T} = 0 \\ \left(\frac{(\lambda+\mu)}{(\lambda+2\mu)}D_1D_2\right)\hat{u}_1 + \left(\frac{\mu}{(\lambda+2\mu)}\Delta + \frac{(\lambda+\mu)}{(\lambda+2\mu)}D_2^2\right)\hat{u}_2 - D_2\hat{T} = 0 \\ -\left(CU^*D_1D_2\right)\hat{u}_1 - \left(CU^*D_2^2\right)\hat{u}_2 + \left(\Delta - U^*D_2\right)\hat{T} = 0 \end{cases} \tag{17}$$

where $U^* = v/C_s$ is the dimensionless velocity. In this work the product of coupling parameter and dimensionless velocity is named, effective coupling parameter $Ce=CU^*$.
The thermal and mechanical boundary conditions which are considered on the material are:

$$T=0, \qquad \text{at} \qquad x=0 \tag{18}$$

$$T=0, \quad \text{at} \quad y=\pm b \tag{19}$$
$$u_1 = u_2 = 0, \quad \text{at} \quad x=0 \tag{20}$$
$$u_1 = u_2 = 0, \quad \text{at} \quad y=\pm b \tag{21}$$
$$\sigma_x = \sigma_{xy} = 0, \quad \text{at} \quad x=l \tag{22}$$
$$q(y,t)=\frac{3Q}{w\sigma'}\exp\left\{-3\left(\frac{y}{\sigma'}\right)^2\right\} \quad \text{at} \quad x=l \tag{23}$$

where w is length of the Gaussian rectangular heat source and σ' is the characteristic (beam) radius (defined as the radius at which the intensity of the laser beam falls to 5% of the maximum intensity[12]).

Finite element method is chosen as a convenient method for solving Eulerian formulation's equations and this modeling is performed with Fortran programming. The geometry is discretized into a number of 6 node triangle elements and the Galerkin finite element technique is used to obtain the solution. The displacements $\hat{u}_1^{(e)}$, $\hat{u}_2^{(e)}$ and temperature $\hat{T}^{(e)}$ are approximated as

$$\hat{u}_1^{(e)}=\sum_{i=1}^{6} N_i\hat{u}_i^*,\ \hat{u}_2^{(e)}=\sum_{i=1}^{6} N_i\hat{v}_i^*,\ \hat{T}^{(e)}=\sum_{i=1}^{6} N_i\hat{T}_i^* \tag{24}$$

Here, N_i is the shape function approximating the displacement and temperature fields in the element (e). Terms, $\hat{u}_i^*$, $\hat{v}_i^*$ and $\hat{T}_i^*$ define the nodal values of displacement and temperature, respectively. Using Eq. (24) and applying the Galerkin finite element method to the governing Eq. (17) for the base element (e), yields:

$$\int_{A^{(e)}}\left[\left\{\frac{\mu}{(\lambda+2\mu)}\Delta+\frac{(\lambda+\mu)}{(\lambda+2\mu)}D_1^2\right\}\hat{u}_1^{*(e)} + \left\{\frac{(\lambda+\mu)}{(\lambda+2\mu)}D_1D_2\right\}\hat{u}_2^{*(e)}-\{D_1\}\hat{T}^{*(e)}\right]N_i\mathrm{dA}=0 \tag{25}$$

$$\int_{A^{(e)}}\left[\left\{\frac{(\lambda+\mu)}{(\lambda+2\mu)}D_1D_2\right\}\hat{u}_1^{*(e)} + \left\{\frac{\mu}{(\lambda+2\mu)}\Delta+\frac{(\lambda+\mu)}{(\lambda+2\mu)}D_2^2\right\}\hat{u}_2^{*(e)}-\{D_2\}\hat{T}^{*(e)}\right]N_i\mathrm{dA}=0 \tag{26}$$

$$\int_{A^{(e)}}\left[-\left\{CU^*D_1D_2\right\}\hat{u}_1^{*(e)} -\left\{CU^*D_2^2\right\}\hat{u}_2^{*(e)}+\{\Delta-U^*D_2\}\hat{T}^{*(e)}\right]N_i\mathrm{dA}=0 \tag{27}$$

Here, $A^{(e)}$ is the surface of the element (e). With the aid of weak formulation:

$$\int_{A^{(e)}}\left[\frac{\partial N_i}{\partial x}\left\{\frac{\partial N_j}{\partial x}\hat{u}_j^*+\frac{\lambda}{(\lambda+2\mu)}\frac{\partial N_j}{\partial y}\hat{v}_j^*-N_j\hat{T}_j^*\right\} +\frac{\mu}{(\lambda+2\mu)}\frac{\partial N_i}{\partial y}\left\{\frac{\partial N_j}{\partial x}\hat{v}_j^*+\frac{\partial N_j}{\partial y}\hat{u}_j^*\right\}\right]\mathrm{dA} +\int_{\Gamma^{(e)}}\left\{\sigma_x n_x+\sigma_{xy}n_y\right\}N_i d\Gamma=0 \tag{28}$$

$$\int_{A^{(e)}}\left[\frac{\partial N_i}{\partial y}\left\{\frac{\partial N_j}{\partial y}\hat{v}_j^*+\frac{\lambda}{(\lambda+2\mu)}\frac{\partial N_j}{\partial x}\hat{u}_j^*-N_j\hat{T}_j^*\right\} +\frac{\mu}{(\lambda+2\mu)}\frac{\partial N_i}{\partial x}\left\{\frac{\partial N_j}{\partial x}\hat{v}_j^*+\frac{\partial N_j}{\partial y}\hat{u}_j^*\right\}\right]\mathrm{dA} +\int_{\Gamma^{(e)}}\left\{\sigma_y n_y+\sigma_{xy}n_x\right\}N_i d\Gamma=0 \tag{29}$$

$$\int_{A^{(e)}}\left[\frac{\partial N_i}{\partial y}\left\{-CU^*\frac{\partial N_j}{\partial y}\hat{v}_j^*-CU^*\frac{\partial N_j}{\partial x}\hat{u}_j^*-U^*N_j\hat{T}_j^*+\frac{\partial N_j}{\partial y}\hat{T}_j^*\right\}+ \frac{\partial N_i}{\partial x}\left\{\frac{\partial N_j}{\partial x}\hat{T}_j^*\right\}\right]\mathrm{dA}+\int_{\Gamma^{(e)}}\left[\left(-CU^*\frac{\partial N_j}{\partial y}\hat{v}_j^*-CU^*\frac{\partial N_j}{\partial x}\hat{u}_j^*- U^*N_j\hat{T}_j^*+\frac{\partial N_j}{\partial y}\hat{T}_j^*\right)n_y+\left(\frac{\partial N_j}{\partial x}\hat{T}_j^*\right)n_x\right]N_i d\Gamma=0 \tag{30}$$

where:

$$\sigma_x=\frac{\partial N_j}{\partial x}\hat{u}_j^*+\frac{\lambda}{(\lambda+2\mu)}\frac{\partial N_j}{\partial y}\hat{v}_j^*-N_j\hat{T}_j^* \tag{31}$$

and

$$\sigma_{xy}=\frac{\mu}{(\lambda+2\mu)}\left\{\frac{\partial N_j}{\partial x}\hat{v}_j^*+\frac{\partial N_j}{\partial y}\hat{u}_j^*\right\} \tag{32}$$

On all the boundary condition except on heated surface the value of the variables (displacement and temperature) are specified. The heated surface is a free traction boundary thus,

$$\sigma_x = \sigma_{xy} = 0 \tag{33}$$

According to the Fourier's law of heat diffusion, on the heated surface,

$$q(y)=-k\frac{\partial T}{\partial x} \tag{34}$$

and according to the dimensionless variables,

$$q(y)=-\frac{kT_o}{\alpha}\frac{\partial T}{\partial x} \tag{35}$$

And notice that on the heated surface $n_y=0$ and $n_x=1$, then the Eqs. 28, 29 and 30 reduce to:

$$\int_{A^{(e)}}\left[\frac{\partial N_i}{\partial x}\left\{\frac{\partial N_j}{\partial x}\hat{u}_j^*+\frac{\lambda}{(\lambda+2\mu)}\frac{\partial N_j}{\partial y}\hat{v}_j^*-N_j\hat{T}_j^*\right\} +\frac{\mu}{(\lambda+2\mu)}\frac{\partial N_i}{\partial y}\left\{\frac{\partial N_j}{\partial x}\hat{v}_j^*+\frac{\partial N_j}{\partial y}\hat{u}_j^*\right\}\right]\mathrm{dA}=0 \tag{36}$$

$$\int_{A^{(e)}}\left[\frac{\partial N_i}{\partial y}\left\{\frac{\partial N_j}{\partial y}\hat{v}_j^*+\frac{\lambda}{(\lambda+2\mu)}\frac{\partial N_j}{\partial x}\hat{u}_j^*-N_j\hat{T}_j^*\right\}+\frac{\mu}{(\lambda+2\mu)}\frac{\partial N_i}{\partial x}\left\{\frac{\partial N_j}{\partial x}\hat{v}_j^*+\frac{\partial N_j}{\partial y}\hat{u}_j^*\right\}\right]dA=0 \quad (37)$$

$$\int_{A^{(e)}}\left[\frac{\partial N_i}{\partial y}\left\{-CU^*\frac{\partial N_j}{\partial y}\hat{v}_j^*-CU^*\frac{\partial N_j}{\partial x}\hat{u}_j^*-U^*N_j\hat{T}_j^*+\frac{\partial N_j}{\partial y}\hat{T}_j^*\right\}+\frac{\partial N_i}{\partial x}\left\{\frac{\partial N_j}{\partial x}\hat{T}_j^*\right\}\right]dA+\int_{\Gamma^{(e)}}\frac{3Q\alpha}{w\sigma' T_o k}\exp\left(-3\left(\frac{y\alpha}{\sigma'}\right)^2\right)N_i dy=0 \quad (38)$$

For Eulerian formulations finite element matrix equations reduce to:

$$[\mathrm{K}]\begin{Bmatrix}\{\hat{\mathrm{u}}_1\}\\{\hat{\mathrm{u}}_2\}\\{\hat{\mathrm{T}}\}\end{Bmatrix}=\begin{Bmatrix}\{\mathrm{F_x}\}\\{\mathrm{F_y}\}\\{\mathrm{Q}\}\end{Bmatrix} \quad (39)$$

Where,

$$[\mathrm{K}]=\begin{bmatrix}\begin{bmatrix}k^{uu}\\k^{vu}\\k^{Tu}\end{bmatrix}&\begin{bmatrix}k^{uv}\\k^{vv}\\k^{Tv}\end{bmatrix}&\begin{bmatrix}k^{uT}\\k^{vT}\\k^{TT}\end{bmatrix}\end{bmatrix} \quad (40)$$

where;

$$k^{uu}{}_{ij}=\int_{A^{(e)}}\left[\frac{\partial N_i}{\partial x}\frac{\partial N_j}{\partial x}+\frac{\mu}{(\lambda+2\mu)}\frac{\partial N_i}{\partial y}\frac{\partial N_j}{\partial y}\right]dA \quad (41)$$

$$k^{uv}{}_{ij}=\int_{A^{(e)}}\left[\frac{\lambda}{(\lambda+2\mu)}\frac{\partial N_i}{\partial x}\frac{\partial N_j}{\partial y}+\frac{\mu}{(\lambda+2\mu)}\frac{\partial N_i}{\partial y}\frac{\partial N_j}{\partial x}\right]dA \quad (42)$$

$$k^{uT}{}_{ij}=\int_{A^{(e)}}\left[-\frac{\partial N_i}{\partial x}N_j\right]dA \quad (43)$$

$$k^{vu}{}_{ij}=\int_{A^{(e)}}\left[\frac{\lambda}{(\lambda+2\mu)}\frac{\partial N_i}{\partial y}\frac{\partial N_j}{\partial x}+\frac{\mu}{(\lambda+2\mu)}\frac{\partial N_i}{\partial x}\frac{\partial N_j}{\partial y}\right]dA \quad (44)$$

$$k^{vv}{}_{ij}=\int_{A^{(e)}}\left[\frac{\partial N_i}{\partial y}\frac{\partial N_j}{\partial y}+\frac{\mu}{(\lambda+2\mu)}\frac{\partial N_i}{\partial x}\frac{\partial N_j}{\partial x}\right]dA \quad (45)$$

$$k^{vT}{}_{ij}=\int_{A^{(e)}}\left[-\frac{\partial N_i}{\partial y}N_j\right]dA \quad (46)$$

$$k^{Tu}{}_{ij}=\int_{A^{(e)}}\left[-CU^*\frac{\partial N_i}{\partial y}\frac{\partial N_j}{\partial x}\right]dA \quad (47)$$

$$k^{Tv}{}_{ij}=\int_{A^{(e)}}\left[-CU^*\frac{\partial N_i}{\partial y}\frac{\partial N_j}{\partial y}\right]dA \quad (48)$$

$$k^{TT}{}_{ij}=\int_{A^{(e)}}\left[-U^*\frac{\partial N_i}{\partial y}N_j+\frac{\partial N_i}{\partial y}\frac{\partial N_j}{\partial y}+\frac{\partial N_i}{\partial x}\frac{\partial N_j}{\partial x}\right]dA \quad (49)$$

where for quadratic triangle element (6 node triangle element),

For the corner nodes:

$$N_1=(2L_1-1)L_1\,,\qquad etc.$$

For the mid-side nodes:

$$N_4=4L_1L_2,\qquad etc.$$

The following exact integration was used to evaluate these integrations.

$$\int\int_A L_1^a L_2^b L_3^c dA=\frac{a!b!c!}{(a+b+c+2)!}2A \quad (50)$$

For the element on the heated surface $\{\mathrm{F_x}\}=\{\mathrm{F_y}\}=0$, and

$$\{\mathrm{Q}\}=\mathrm{Q_i}=\int_{\Gamma^{(e)}}\frac{3Q\alpha}{w\sigma' T_o k}\exp\left(-3\left(\frac{y\alpha}{\sigma'}\right)^2\right)N_i dy=0 \quad (51)$$

where N_i are the shape functions of the elements' nodes which place on the heated surface.

III. Analytical Model

An analytical model, based on the renowned transient heat conduction equation, was used to describe the temperature distribution as a function of time and step T(r,t) in the material under the action of a laser beam that move with different moving pattern:

$$\rho c_p\frac{\partial T}{\partial t}+\nabla(-K\nabla T)=f(r,t) \quad (52)$$

where ρ, cp and K are, the density, specific heat and thermal conductivity of the material. The internal heat generation term $f(r,t)$, at the right side of Eq. (52), is identified as the energy distribution of the laser beam.

If ρ, cp and K are temperature and position independent, Eq. (52) is taken in the form,

$$\frac{1}{\kappa}\frac{\partial T}{\partial t}-\nabla^2 T=\frac{f(r,t)}{K} \quad (53)$$

Where $\kappa = K/\rho\, c_p$ is the thermal diffusivity.

In the case of three-dimensional transient problem, given by equation (53), the solution for $T(\mathrm{r},\mathrm{t})$ is expressed in terms of the three-dimensional Green's function [11],

$$T(\mathbf{r},t)=\frac{\kappa}{K}\int_{\tau=0}^{t}d\tau\int_R G(\mathbf{r},t\mid\mathbf{r}',\tau)f(\mathbf{r}',\tau)dv'+\int_R G(\mathbf{r},t\mid\mathbf{r}',\tau)|_{\tau=0}\;F(\mathbf{r}')dv' \quad (54)$$

where $F(\mathbf{r}')$ is the initial temperature distribution.

The three-dimensional Green' function can be obtained from the product of the three one-dimensional Green' function as in rectangular coordinates:

$$G1(x,y,z,t\mid x',y',z',\tau)=G1(x,t\mid x',\tau)\times G2(y,t\mid y',\tau)\times G3(z,t\mid z',\tau) \quad (55)$$

In the case of two-dimensional transient problem the two-dimensional T(r,t) is expressed in terms of the two-dimensional Green's function. The two-dimensional Green' function can be obtained from the product of the two one-dimensional Green' function as,

$$G1(x,y,t\mid x',y',\tau)=G1(x,t\mid x',\tau)\times G2(y,t\mid y',\tau) \quad (56)$$

where each of the one-dimensional Green's functions depends on the extent of the region (i.e. , finite, semi infinite, or infinite) and the boundary conditions, where the one-dimensional infinite medium Green's function obtain as [11],

$$G(y,t\mid y',\tau)=\left[4\pi\alpha(t-\tau)\right]^{-1/2}\exp\left(-\frac{(y-y')^2}{4\alpha(t-\tau)}\right) \quad (57)$$

And the semi infinite medium when the boundary at $x=l$ is of the second kind (insulate) Green's function obtains as [11]:

$$G(x,t\mid x',\tau)=\left[4\pi\alpha(t-\tau)\right]^{-1/2}\cdot\left[\exp\left(-\frac{(x-x')^2}{4\alpha(t-\tau)}\right)+\exp\left(-\frac{(x+x')^2}{4\alpha(t-\tau)}\right)\right] \quad (58)$$

Substituting $G1$ and $G2$ in Eq. (56) yields the two-dimensional Green's function, for $x'=0$,

$$G(x,y,t\mid x',y',\tau)=2\left[4\pi\alpha(t-\tau)\right]^{-1}\times\exp\left(-\frac{(y-y')^2+x^2}{4\alpha(t-\tau)}\right) \quad (59)$$

And also the three dimensional Green's function obtain as, for $x'=0$,

$$G(x,y,z,t\mid x',y',z',\tau)=2\left[4\pi\alpha(t-\tau)\right]^{-1.5}\times\exp\left(-\frac{(y-y')^2+(z-z')^2+x^2}{4\alpha(t-\tau)}\right) \quad (60)$$

Then the 2 dimensional temperature distribution obtain,

$$T(x,y,t)=T_o+\frac{\alpha}{K}\int_0^t\int_{-\infty}^{\infty}f(y',\tau).2[4\pi\alpha(t-\tau)]^{-1}.\exp\left(-\frac{(y-y')^2+x^2}{4\alpha(t-\tau)}\right)dy'\,d\tau \quad (61)$$

and 3 dimensional temperature distribution obtain,

$$T(x,y,z,t)=T_o+\frac{\alpha}{K}\int_0^t\int_{-w}^{w}\int_{-\infty}^{\infty}f(y',\tau).2[4\pi\alpha(t-\tau)]^{-1.5}\exp\left(-\frac{(y-y')^2+(z-z')^2+x^2}{4\alpha(t-\tau)}\right)dy'dz'd\tau \quad (62)$$

In this equation, $f(y',\tau)$ is the beam intensity distribution, which for a beam with Gaussian distribution that move along a straight line is taken the form,

$$f(y',\tau)=\frac{3Q}{w\sigma'}\exp\left\{-3\left(\frac{y'-v\tau}{\sigma'}\right)^2\right\} \quad (63)$$

IV. NUMERICAL EXAMPLE

To compare the results of the method presented in this paper, a rectangular (30 mm along the direction of laser moving and 10 mm thickness) of AISI 1045 steel was considered as shown in Fig. 1 Laser processing parameters that used in the comparison studies are Q=450W, w=10mm and $\sigma'=1.5mm$.

At the beginning a study was performed to compare the result of two dimensional uncouple analytical equation (Eq.61) with the result of the three dimensional uncouple analytical equation (Eq.62) to ensure that the thermal field for this intensity distribution can be analyzed in two dimensional. Figure 2 shows the dimensionless temperature changes with time at a point on the heated surface, which was obtained from two and three dimensional uncoupled analytical equations 61 and 62. As shown in Fig. 2 the two dimensional analysis result is in good agreement with the three dimensional analysis result so, the thermal field can be analyzed as a two dimensional heat conduction problem.

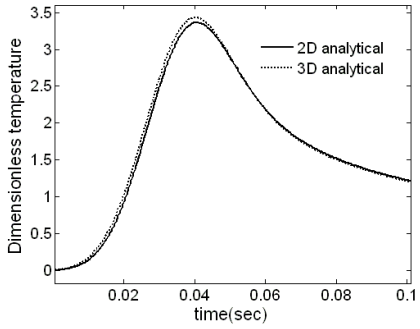

Fig. 2 The dimensionless temperature histories of a point on the heated surface

Fig. 3 shows a comparison of the dimensionless temperature changes along y direction on the heated surface. Fig. 4 shows a comparison of changes of the dimensionless displacement in X direction along scan path on the heated surface. The results are plotted for different effective coupling parameters

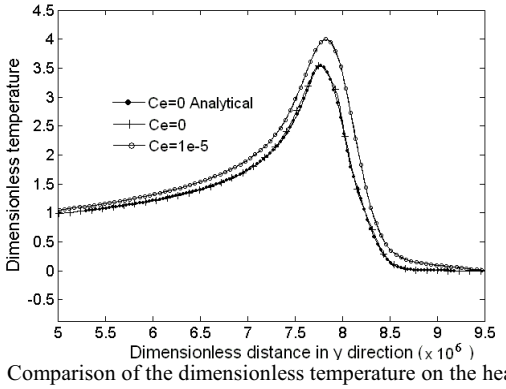

Fig. 3 Comparison of the dimensionless temperature on the heated surface

The case of *Ce=0* corresponds to the uncoupled solution. The coupled results are presented for *Ce=1e-5*.As shown the Eulerian formulations thermal results, are in good agreement with the analytical result in the case of uncoupled solution *(Ce=0)*.

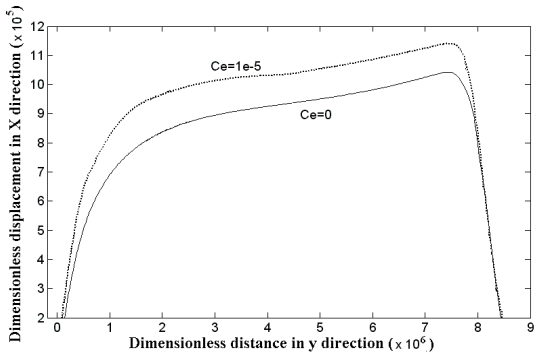

Fig. 4 Comparison of the dimensionless displacement in x direction on the heated surface

As shown in Figs. (3) and (4) the coupled temperature and displacement are more than the temperature and displacement, which are driven from uncoupled theory (*Ce=0*). So the coupling acts as a power generator in the system.

Fig. 5 shows the contours of the dimensionless stress Sx and corresponding values for different effective coupling parameter (a) *Ce=0* (b) *Ce=1e-5* in the heated region and again the case of *Ce=0* corresponds to the uncoupled solution.

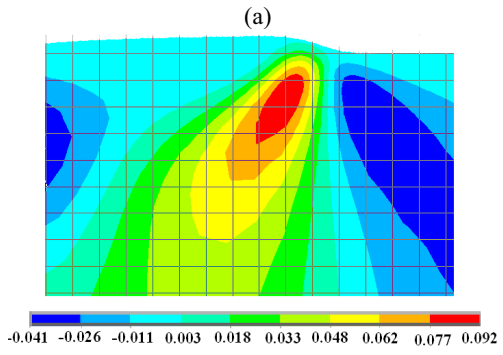

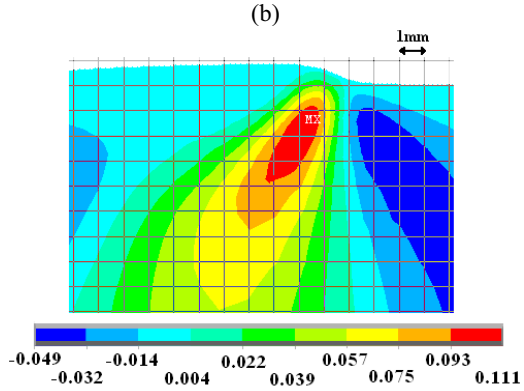

Fig. 5 Contours of the dimensionless stress S_x for effective coupling parameters (a) Ce=0 (b) Ce=1e-5 in the heated region.

During the heat-up the local severe temperature gradients in the vicinity of the heat affected zoon causes thermal expansion of the material in this region but this material is constrained by the surrounding material. The constraint leads to compressive stresses in X and Y directions in this region and near the heated surface which exceeding yield stress within the target material.

Fig. 6 shows the contours of the dimensionless stress Sy and corresponding values for different effective coupling parameter (a) *Ce=0* (b) *Ce=1e-5*. As shown in Fig. 6 the local severe temperature gradients in the vicinity of the heated region produces compressive stresses in Y direction. However, the thermal stress state changes to the tensile stress as the distance from the centre line increases.

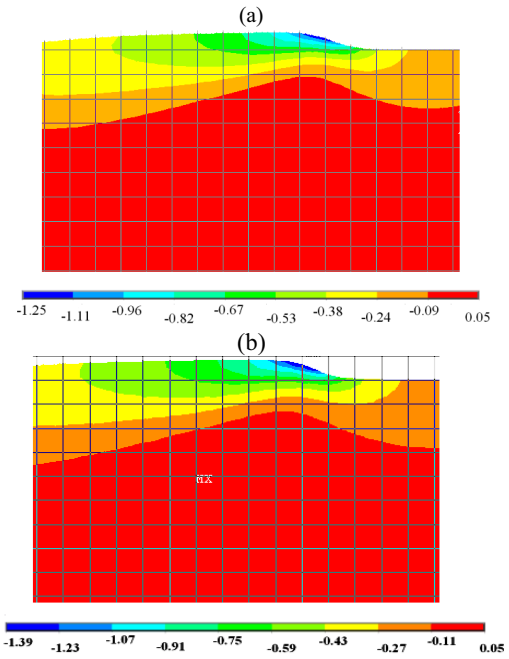

Fig. 6 Contours of the dimensionless stress S_y for effective coupling parameters (a) Ce=0 (b) Ce=1e-5 in the heated region.

Coupling parameter for AISI 1045 steel

In this section, the coupling parameter for surface treatment of 1045 steel was studied. Realistic effects like temperature dependent thermal and mechanical properties, phase transformation are included in this study.

The temperature-dependent mechanical properties of AISI 1045 steel from Ref. [11] were chosen and the temperature-dependent thermal properties of AISI 1045 steel are accepted from Ref. [13]. The thermal expansion coefficient α was accepted from ref [15]. The beginning of the austenitic transformation temperature range 830 ^{o}C was considered and the end of austenitic transformation temperature range 950 ^{o}C was considered [16, 12]. The volume changes of the austenitic transformation were considered by equivalent linear thermal expansion coefficient and 2.5×10^{-3} were adopted which is a little less than the thermal expansion coefficient (2.8×10^{-3}) that was used in Ref. [17] to avoiding negative specific heat at constant strain. Fig. 7 shows the changes of specific heat at constant strain with time which is computed from Eq. (3).

In Fig. 8 the changes of effective Coupling parameter versus temperature for laser velocity of 40 mm/sec is shown.

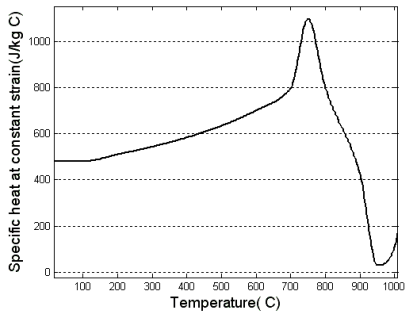

Fig. 7 Specific heat at constant strain of AISI 1045 versus temperature

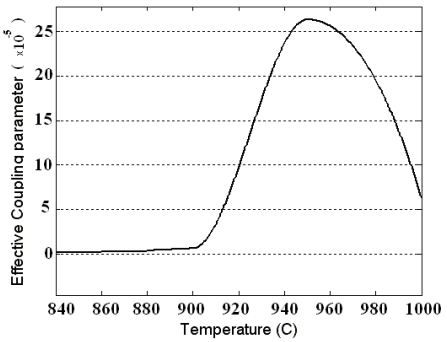

Fig. 8 Effective Coupling parameter for surface hardening of 1045 steel versus temperature

V. Conclusions

A finite element model is developed for the calculation of thermoelastic temperature, displacement and stress fields in a thermoelastic solid which subjected to thermal load from a moving laser beam. The thermal and mechanical fields are assumed to be coupled. For constant velocity and heat flux distribution, the Eulerian formulations leads to a steady-state problem. The Eulerian formulations thermal results are in good agreement with the analytical result in the case of uncoupled solution *(Ce=0)*. The result show that coupled temperature and displacement are more than the temperature and displacement, which are driven from uncoupled theory (*Ce=0*). So the coupling acts as a power generator in the system.

References

[1] Peyre P, Fabbro R, Berthe L, Dubouchet C. Laser shock processing of materials. J Laser Appl 1996;8:135–41.
[2] Welsh, L.P.,Tuchmqn, J.A.,and Herman, J.P., The importance of thermal stresses and strains induced in laser processing with focused Gaussian beam ,J. Appl. Phys., Vol. 64, p.6274, 1988.
[3] K.D. Schwager, B.Scholes, E.Macheraunch,and B.L.Mordike, Proc.ECLAT 92,DGM,pp.629-634
[4] M.Bouffoussi, S.Denis, J.Ch.Chevrier, A. Simon, A. Bignonnet, and J. Merlin, Proceedings of European Conference on laser Treatment of metals, ECLAT 92 DGM, 1992,pp.635-640.
[5] Germanovich, L. N.,Kill, I. D., and Tsodokova, n.s., Thermoelasstic stresses in a half-space heated by concentrated energy flux, J. of Applied Mech., Vol. 52, P. 525, 1989.
[6] P. Hosseini-Tehrani, M.R. Eslami, BEM analysis of thermal and mechanical shock in a two-dimensional finite domain considering coupled thermoelasticity, Engineering Analysis with Boundary Elements 24 (2000) 249–257.
[7] S. M. Rajadhyaksha and P. Michaleris, Optimization of thermal processes using an Eulerian formulations and application in laser surface hardening, Int. J. Numer. Meth. Engng. 2000; 47:1807-1823.
[8] P. Hosseini-Tehrani, M.R. Eslami, Boundary element analysis of stress intensity factor KI in some two-dimensional dynamic thermoelastic problems, Engineering Analysis with Boundary Elements 29 (2005) 232–240.
[9] ASYS Help System, Theory Reference , Ver. 10.
[10] Bagri, M.R. Eslami, Generalized coupled thermoelasticity of functionally graded annular disk considering the Lord–Shulman theory, Composite Structures xxx (2007).
[11] Andrei D. Polyanin, Handbook of linear partial differential equations for engineers and scientists, 2002.
[12] Y. S. Yang and S. J. NA, A study on residual stresses in laser surface hardening of a medium carbon steel, surface and coatings technology, 38(1989) 311-324.
[13] Tan Zhen, Guo Guangwen, editors. Thermo-physical properties of engineering alloy. Publishedby Metallurgical industry Publisher; 1994. 9pp.
[14] X.F. Wanga,b, X.D. Lua, G.N. Chenb, Sh.G. Hua, Y.P. Sua, Research on the temperature field in laser hardening, optics & Laser Technology 38 (2006) 8–13.
[15] ASM International, ASM Handbook: properties and selection, vol. 1, ASM International, 1994
[16] S. J. Na and Y. S, Yang, Influence of heating rate on the laser surface hardening of a medium carbon steel, surf. Coat. Technol., 34 (1988) 319-330.
[17] T. Inue and K. Tanaka, An elastic-plastic stress analysis of quenching when considering a transformation, Int. J. Mech. Sci., 17 (1975) 361 – 367.